Purification and characterization of hypo-glycosylated $hFSH^{21}$ and fully-glycosylated $hFSH^{24}$.

Supplement to: **Hypo-glycosylated Human Follicle-Stimulating Hormone ($hFSH^{21/18}$) is much more active *in vitro* than fully-glycosylated hFSH ($hFSH^{24}$).**

George R. Bousfield[1], Vladimir Y. Butnev[1], Viktor Y. Butnev[1], Yasuaki Hiromasa[2], David J. Harvey[3], and Jeffrey V. May[1]

1. Introduction

This supplement provides detailed procedures for the studies in the accompanying manuscript and results of detailed biochemical analysis of two hFSH glycoform preparations employed in receptor-binding studies. The naturally occurring hypo-glycosylated variant, $hFSH^{21/18}$, was isolated from purified hLH preparations. A fully-glycosylated, $hFSH^{24}$ preparation, was reconstituted from hCGα and HPLC-purified $hFSH\beta^{24}$ subunit preparations.

2. Methods

2.1 Hypo-glycosylated hFSH isolation

Batches of 100 mg hLH were dissolved in 5 ml 0.1 M sodium phosphate buffer, 0.3 M sodium chloride, pH 7.0, and subjected to three rounds of FSH immunopurification using immobilized anti-hFSHβ monoclonal, 46.3H6.B7 (Bousfield, Butnev, Walton et al., 2007). The hLH solution was recycled three times through three, 1-ml 46.3H6.B7 antibody columns at a flow rate of 1 ml/min. After the third pass, the column inlet was removed from the sample tube and inserted into the loading buffer reservoir. Unbound protein collection continued until the absorbance had almost returned to baseline. The columns were then washed with additional loading buffer for 20 min. Bound protein was eluted with 0.2 M glycine-HCl, 0.5 M NaCl buffer, pH. 2.7, and collected in a 10,000 MW cutoff, Amicon (Millipore, Bilerica, MA) Ultra-4 ultrafiltration cartridge containing 400 μl 1 M Tris-HCl, pH 9.5. After mixing by inversion, the 4-ml total volume was reduced to 100-200 μl by centrifugation at 4000 X g for 20 min in the H-6000A rotor of a Sorvall (Thermo Fisher Scientific, Inc, Waltham, MA) RC-3B Plus refrigerated

centrifuge at 4°C. The retained fraction was applied to a 10 X 300 mm Superdex 75 column that was equilibrated with 0.2 M ammonium bicarbonate/20% acetonitrile. The Waters (Milford, MA) HPLC system consisted of a model 717 refrigerated autosampler, model 626 quaternary gradient pump, model 600E pump controller, and model 486 programmable variable wavelength monitor. The components were controlled by and data obtained with Waters Empower software running on a Dell (Round Rock, TX) model 8250 computer. The chromatogram was developed with the 0.2 M ammonium bicarbonate/20% acetonitrile buffer at 0.4 ml/min at 25°C. Fractions were collected by hand and protein recovered by evaporation in a Savant (Thermo Scientific, Waltham, MA) Speed Vac. An aliquot of 300 μl Milli-Q (Millipore, Bilerica, MA) water was added to each dried tube and evaporation repeated. Dried tubes were stored at -20°C until use.

2.2 Fully-glycosylated hFSH assembly from purified subunit preparations

As no efficient method existed for glycoform separation, we assembled easily purified fully-glycosylated hFSHβ[24] with a readily available α subunit preparation, hCGα. A partially purified hFSHβ[24] preparation was subjected to reverse-phase HPLC using a 4.6 X 250 mm Vydac (Grace, Deerfield, IL) C18 column connected to the Waters HPLC system described above. The column was equilibrated with 0.1% TFA/water at a flow rate of 1 ml/min. The subunit preparation was dissolved in 0.1% TFA/water and applied to the column. The chromatogram was developed under initial conditions for 10 min, then with a gradient to 20% acetonitrile containing 0.1% TFA over 20 min, followed by a gradient to 40% acetonitrile/TFA over 10 min. After 5 min at the final conditions, the column was equilibrated with 0.1% TFA/water. Fractions were collected by hand and 24,000 M_r hFSHβ recovered from the peak emerging at 27.4 min by evaporation in a SpeedVac. The hCGα subunit was derived from hCG dissociated in 6 M GuHCl by overnight incubation at 37°C. Subunits were separated by Sephacryl S-200 gel filtration. A 874 μg sample of 24,000 M_r hFSHβ and a 2650 μg sample of hCGα were dissolved in 0.5 M Tris-acetate, pH 6.0, containing 0.05% sodium azide, and incubated 72 hr at 37°C. The volume was then reduced to less than 200 μl by Amicon Ultra-4 centrifugal ultrafiltration. The entire sample was applied to a 10 X 300 mm Superdex 75 gel

filtration column. The chromatogram was developed with 0.2 M ammonium bicarbonate/20% acetonitrile, at a flow rate of 0.4 ml/min. Fractions were collected by hand and protein recovered by evaporation in the SpeedVac. Here we note that we also prepared fully-glycosylated hFSH by combining 24,000 M_r hFSHβ with hFSHα. However, as some 21,000 M_r hFSHβ contaminating the hFSHα preparation was introduced into the resulting heterodimer preparation, we did not employ it in these studies.

2.3 Molecular weight determination by gel filtration

Either one or two, 10 X 300 mm Superdex 75 columns were coupled to a HPLC system consisting of a Waters model 717 plus autosampler, model 625 quaternary gradient HPLC pump, and model 486 programmable absorbance monitor. HPLC control and data acquisition employed the same Empower software used above. The mobile phase was 0.2 M ammonium bicarbonate containing 20% acetonitrile at a flow rate of 0.4 mL/min for 70 min (one column) or 140 min (2 columns). One μg samples of each glycoform preparation were injected and chromatograms developed for each injection. These were followed by separate injections of samples containing a mixture of both preparations. Molecular weight markers, bovine serum albumin, ovalbumin, ribonuclease A, aprotinin, and vitamin B12 (Sigma/Aldrich, St. Louis, MO), were used to calibrate the column(s).

2.4 Hypo-glycosylated hFSH$^{21/18}$ total glycan analysis by mass spectrometry

A 13.1 μg sample of hypo-glycosylated hFSH$^{21/18}$ was reduced and carboxymethylated, then desalted and buffer replaced with 0.2 M ammonium bicarbonate, pH 8.5, by means of Amicon Ultra-4 centrifugal ultrafiltration. The protein was digested overnight with 2.5 mU PNGaseF in 0.2 M ammonium bicarbonate, pH 8.5. Completion of deglycosylation was confirmed by Superdex 75 gel filtration of a 1 μg sample. Oligosaccharides were separated from the remaining digest by reverse-phase HPLC and recovered by evaporation in a SpeedVac. The oligosaccharide sample was analyzed by nano-electrospray mass spectrometry performed with a Waters quadrupole-time-of-flight (Q-TOF) Ultima Global instrument in negative ion mode. Samples in 1:1 (v:v) methanol:water containing 0.5 mM ammonium phosphate were infused

through Proxeon nanospray capillaries (Proxeon Biosystems, Odense, Denmark). The ion source conditions were: temperature, 120°C; nitrogen flow 50 L/hr; infusion needle potential, 1.1 kV; cone voltage 100 V; RF-1 voltage 180 V. Spectra (2 sec. scans) were acquired with a digitization rate of 4 GHz. For MS/MS data acquisition (collision-induced decomposition, CID), the parent ion was selected at low resolution (about 5 *m/z* mass window) to allow transmission of isotope peaks and fragmented with argon at a pressure (recorded on the instrument's pressure gauge) of 0.5 mBar. The voltage on the collision cell was adjusted with mass and charge to give an even distribution of fragment ions across the mass scale and spectra were accumulated until a satisfactory signal:noise ratio had been obtained. Typical values were 80-120 V. Other voltages were as recommended by the manufacturer. Instrument control, data acquisition and processing were performed with MassLynx software Version 4.0.

2.5 Spectral interpretation

The mass of the glycans gave the composition in terms of the constituent isobaric monosaccharides. Structural details were obtained by fragmentation. Negative ion CID spectra of neutral *N*-glycans provide much more structural detail than the more commonly used positive ion spectra and were used for all samples. Major ions define features such as the branching pattern, the location of fucose residues and the presence or absence of bisecting GlcNAc. Full details have been published (Harvey, 2005). The glycans were stabilized for negative ion work by adduction with a low mass anion, phosphate in this case, because phosphate always appears to be present in glycan samples obtained by release from glycoproteins, even after extensive clean-up. The anion does not affect the CID spectra because it is lost in the first fragmentation event. The corresponding spectra of acidic (sialylated and sulfated) glycans, which ionize as $[M-H]^-$ ions and do not form adducts, are not so informative because of preferential loss of the acidic protons during fragmentation. Therefore, the analytical method that was adopted was to perform structural analysis on the desialylated glycans and then to use the spectra of the native glycans to determine the sialylation state of each compound. Consequently, in the composition tables below, the glycans are listed in order of their neutral masses with the number and masses of the

acidic groups in the columns following the neutral structure. Time did not permit fragmentation of all compounds in every sample but enough data were collected to assign structures to most glycans.

2.6 Quantitative MS data

Quantitative data were obtained for hypo-glycosylated hFSH glycans by adding the peak heights of all isotopes for each compound and expressing the result as a percentage of the total ion count (Harvey, Royle, Radcliffe et al., 2008). Although this method gives an approximate indication of the amounts of each glycan it will not be totally accurate for a number of reasons. (a) Compounds ionize in different states ($[M-H]^-$ and $[M-2H]^{2-}$ for acidic glycans and $[M+H_3PO_4]^-$ for the neutral compounds) and the relative ionization efficiency for production of each ion is unknown, (b) Some ions contain isomeric and isobaric structures and it is sometimes not possible to determine the contribution of each to the ion current. In some cases, however, this can be estimated from the fragmentation spectra. Amounts are cited to two places of decimals: this is to define the dynamic range, not the accuracy.

Comparison of glycan populations was performed by summing the negative ion mode abundance data for charge variants of each neutral core structure associated with either the hypo-glycosylated $hFSH^{21/18}$ or pituitary $hFSH^{24/21}$ preparation. The data for the former are reported herein, while the data for the latter are contained in a separate report (Bousfield et al. submitted). This permits comparison of glycan population by specific glycan type. Not shown, but available in the appropriate tables are differences in sialic acid and sulfate content shown in the negative ion mode tabular data.

2.7 FSH iodination

FSH preparations were iodinated by the chloramine T method, as described previously (Bousfield and Ward, 1984). The specific activities were 39-41 μCi/μg. For competition and association studies, ^{125}I-labeled FSH preparations were diluted to 25 ng/ml and stored at 4°C until use.

2.8 Rat testis RLA

The Wichita State University institutional animal care and use committee approved all animal procedures. Male rats were sacrificed by CO_2 asphyxiation and their testicles removed, decapsulated, weighed, and homogenized in 4 volumes RLA buffer consisting of 0.1 M Tris-HCl, pH 7.5 containing 0.1% bovine serum albumin. FSH receptor binding was tested using 25 mg/tube rat testis homogenate and either ^{125}I-hFSH$^{21/18}$ or ^{125}I-hFSH^{24} preparations. Each assay tube received 2.5 ng ^{125}I-FSH tracer. For saturation studies, half of the iodinated hFSH glycoform preparation was diluted separately to provide a series of concentrations ranging from 0.464 to 464 ng/ml. These were incubated in the presence of increasing concentrations of cold eFSH[18], hFSH$^{24/21}$, and hFSH glycoform preparations at 37°C for 2 hr. The tubes were then placed in the H-6000A rotor of an RC-3B Plus centrifuge and centrifuged at 3500 x g for 20 min at 4°C. The supernatants were aspirated and bound hormone in the pellets counted in a Packard (Perkin Elmer, Waltham, MA) Cobra II gamma counter. The counting efficiency was 74%.

2.9 Saturation binding of FSH to rat testis homogenate

Increasing concentrations of ^{125}I-hFSH and FSH glycoform preparations were added to 12 X 75 mm tubes with or without 2000-fold excess cold FSH. Rat testis homogenate was added to each tube and all the tubes incubated for 2 hr at 37°C with constant shaking. The tubes were centrifuged for 20 min at 3500 rpm in the H-6000A rotor of an RC-3B plus centrifuge. The supernatant was aspirated and ^{125}I-tracer bound to the pellet was counted in the gamma counter. Specific binding was calculated by subtracting cpm in nonspecific binding tubes from cpm from the corresponding total binding tubes and specific binding plotted against hormone concentration. Saturation curves were plotted using the GraphPad (San Diego, CA) software package Prism (v5.0c).

2.10 Association kinetics in rat testis homogenate

Tubes containing 2.5 ng ^{125}I-hFSH tracer and 25 mg rat testis homogenate were incubated at 37°C for various times. Following incubation, the tubes were place in an ice bath and kept at 4°C until all the incubations were completed. Once the last tube was placed on ice, all tubes were

placed in the H-6000A rotor of the RC-3B plus centrifuge and centrifuged for 20 min at 3500 rpm. The supernatants were aspirated and the bound ^{125}I-hFSH measured in the gamma counter.

2.11 Hypo-glycosylated FSH$^{21/18}$ subunit isolation

Since reverse-phase HPLC cannot isolate hFSHβ^{21} subunit, FSH subunits in the post-dimer fraction derived from hFSH$^{21/18}$ Superdex 75 chromatograms were separated by immunoaffinity chromatography using FSHβ-specific monoclonal antibody, 46.3H6.B7 (Walton, Nguyen, Butnev et al., 2001) followed by Superdex 75 gel filtration of the bound (hFSHβ$^{21/18}$) and unbound (hFSHα) fractions. The subunit fractions were characterized by automated Edman degradation and carbohydrate composition analysis.

2.12 Carbohydrate analysis of purified hypo-glycosylated hFSH$^{21/18}$ subunit preparations

Samples consisting of 6 μg of either hFSHβ$^{21/18}$ or hFSHα were dried in separate 2-ml polypropylene screw-cap microcentrifuge tubes, then hydrolyzed in 200 μl 4 N TFA for 4 hr at 100°C. The hydrolysates were dried in the SpeedVac and dissolved in 100 μl water. Duplicate 10 μl aliquots were analyzed in a Thermo Scientific, Dionex (Sunnyvale, CA) ISC-5000 carbohydrate analyzer equipped with a PA-20 CarboPac column equilibrated with 10 mM NaOH at a flow rate of 0.5 ml/min and temperature of 30°C. Monosaccharide chromatograms were developed under the same conditions for 12 min. The chromatogram was developed with 200 mM NaOH for 10 min to remove peptide components of the hydrolysate, then re-equilibrated with 10 mM NaOH for 10 min prior to injection of the next sample. The carbohydrate analyzer was controlled by and electrochemical detector signals captured with the Dionex software package, Chromeleon v 6.8, running on a Dell Optiplex 780 computer.

2.13 Glycoform glycosylation evaluation by PNGase, SDS-PAGE, and PAS-staining

Three μg samples of each hFSH preparation were dried in 0.5 ml microfuge tubes. Each sample was dissolved in 47.5 μl 0.1% SDS, 50 mM 2-mercaptoethanol, and boiled for 5 min at 100°C. The nonionic detergent, NP-40 was added to a final concentration of 0.75% to neutralize the denaturing effect of SDS. Finally, 0.4 μl (1 mU) aliquots of Prozyme (Hayward, CA) N-Glycanase® (peptide-N-glycanase F; PNGaseF) were added and the samples incubated overnight

at 37°C. Following incubation the samples were dried and dissolved in 30 μl Laemmli SDS sample buffer and boiled for 3 min. Each gel well received 1 μg hFSH. SDS-PAGE was carried out on 8-16% polyacrylamide gradient gels (BioRad Ready Gel) at 200 V for 1 hr. Proteins were transferred to PVDF membranes and probed with monoclonal antibodies RFSH20 (anti-FSHβ) and HT13 (anti-α subunit).

2.14 Matrix Assisted Laser Desorption Ionization Time-Of-Flight (MALDI-TOF) mass spectrometry

MALDI-TOF mass spectrometry measurements were performed using a Bruker Ultraflex II TOF/TOF instrument (Bruker Daltonics, Bremen, Germany) operating in the linear and positive modes. Ions formed with a nitrogen pulse laser beam were accelerated to 25 kV. Sinapinic acid (Sigma-Aldrich, St. Louis, MO) was used as a matrix. MS spectra were recorded within a mass range from *m/z* 10,000 to *m/z* 20,000 and externally calibrated using a protein mass standard kit I in the *m/z* range of 5,734.5 (insulin) to 16,952.3 (Bruker Daltonics, Billerica, MA).

3. Results and Discussion

3.1 Molecular size analysis of glycoform preparations by gel filtration chromatography

FSH concentrations in hypo- and fully-glycosylated hFSH preparations were quantified by gel filtration using a 10 X 300 mm Superdex 75 column, which has been used by others for measuring concentrations of highly purified hFSH preparations (Louriero, de Oliveira, Torjesen et al., 2006,Stanton, Robertson, Burgon et al., 1992). During these experiments, we noticed retention times for hypo- and fully-glycosylated hFSH were 28.6 and 27 min, respectively, which corresponded to molecular weights of 23,483 and 33,660 (data not shown). The former mass was 12% less and the latter was 7% more than the sum of the α and β subunit masses determined by MALDI-MS of hFSH glycoforms (*m/z* 26,773 for $hFSH^{21/18}$ and 31,502 for $hFSH^{24}$) (Bousfield et al., 2007). Partially overlapped, individual glycoform chromatograms gave the impression that at least partial glycoform resolution was possible. However, injection of a sample containing both glycoform preparations produced only a single peak, with a retention time of 26.5 min,

corresponding to a molecular weight of 37,668. The single FSH peak was consistent with our experience that $hFSH^{24/21}$ preparations emerged as a single peak during purification of single-pituitary, immunoaffinity-purified hFSH $hFSH^{24/21}$ heterodimer with single 10 x 300 mm Superdex 75 columns (Bousfield et al., 2007).

Based on the report of Flack et al. (Flack, Froehlich, Bennet et al., 1994) showing different retention times for mutant recombinant hFSH preparations possessing 2, 3, or all 4 N-glycans following chromatography on two 1.6 x 80 cm Sephadex G-75 columns connected in series, we coupled two 10 X 300 mm Superdex 75 columns to increase the separation of FSH glycoforms. The retention time difference between glycoforms increased to 4.2 min (Figs. 1A & 1B). When samples of both glycoforms were combined and chromatographed, two peaks emerged, and each could be integrated (Fig. 1C). The peak heights were different, as $hFSH^{21/18}$ preparations appeared to suffer losses when samples were dried. The molecular weights for $hFSH^{21/18}$ and $hFSH^{24}$ were determined to be 37,700 and 57,500, respectively, which were 41% to 83% greater than the combined subunit masses determined by MALDI-MS (*m/z* 26,773 for $hFSH^{21/18}$ and 31,502 for $hFSH^{24}$). Gonadotropin molecular weights determined by gel filtration are typically greater than their masses because both subunits are elliptical in shape (Fox, Dias and Van Roey, 2001) and both molecular shape and glycan modifications influence gel filtration behavior (Siegel and Monty, 1966).

3.2 Hypo-glycosylated $hFSH^{21/18}$ glycans

PNGaseF-released oligosaccharides from reduced, carboxymethylated $hFSH^{21/18}$ were characterized by nano-ESI-MS. The MS spectra (Fig. 2) revealed considerable heterogeneity in the intact glycan, negative ion spectrum, as 46 neutral compounds corresponding to the core glycans, and 43 negatively charged variants of 27 complex core structures were observed (Table 3 and Fig. 3). At least 45 core structures were identified in the desialylated glycan spectrum. The intact and desialylated glycan spectra were very similar because 60% of the oligosaccharides were oligomannose structures that possessed 3-9 mannose residues and lacked terminal sialic acid residues. The ions representing these species were present in both spectra, as neuraminidase

digestion had no effect on glycans lacking sialic acid. The unusually high abundance of oligomannose glycans was the most striking feature of the hypo-glycosylated $hFSH^{21/18}$ glycan population, as the abundance of these glycans was generally reported to be low in other highly purified pituitary hFSH preparations (Bousfield, Butnev, Bidart et al., 2008,Dalpathado, Irungu, Go et al., 2006,Green and Baenziger, 1988,Renwick, Mizuochi, Kochibe et al., 1987). A comparison of the hypo-glycosylated $hFSH^{21/18}$ glycan population with that derived from highly purified pituitary $hFSH^{24/21}$ glycans that were also analyzed using the same analytical procedures is shown in Fig. 4. The bulk of the $hFSH^{21/18}$ oligomannose glycans were either undetectable or very low abundance in the pituitary $hFSH^{24/21}$ glycan population. The complex glycans typical of the latter preparation were either very low in abundance or undetectable in hypo-glycosylated $hFSH^{21/18}$. Thus, purification of hypo-glycosylated hFSH from hLH preparations revealed an additional form of FSHβ macroheterogeneity resulting in the $hFSH\beta^{18}$ band, as well as a unique pattern of microheterogeneity not seen in other hFSH preparations.

3.3 Subunit characterization

Hypo-glycosylated $hFSH^{21/18}$ subunits were separated by immunoaffinity chromatography and desalted by gel filtration (Fig. 5). As Western blotting of the subunit fraction prior to removal of α subunit had revealed the presence of both 18,000 and 21,000 M_r bands (manuscript Fig. 2, inset 1, lane 4), a sample of the $hFSH\beta^{21/18}$ preparation was analyzed by MALDI-MS (Fig. 6B). Two major components were detected. At the low mass end of the spectrum, a signal with a maximum at *m/z* 12,601 indicated the presence of some non-glycosylated hFSHβ, as the formula weight for the hFSHβ protein moiety is 12,485. The spectrum in this region was not as well-defined as that collected several years ago on a different instrument for a sample of $hFSH\beta^{21}$ in which two major ions were detected, *m/z* 12,361 and 12,567 (Walton et al., 2001). A second broad region of overlapping ions with a maximum intensity at 13,623 *m/z* was lower than a singly-glycosylated eFSHβ variant, *m/z* 14,332 (Bousfield, Butnev, Gotschall et al., 1996). The hFSHα subunit preparation appeared as a broad signal with an intensity maximum at 12,667 *m/z*. It's presence would have interfered with the *m/z* 12,601 signal from hypo-glycosylated hFSHβ if

intact hFSH had been analyzed, as reported previously (Bousfield et al., 2007). As noted above, carbohydrate analysis of the hypo-glycosylated hFSH–associated subunit preparations confirmed the presence of both complex and oligomannose glycans (manuscript Table 2) revealed by the mass spectrometry data (Figs. 2 & 3). The α subunit possessed 81% more glycan than FSHβ, consistent with the quantitative glycosylation of the common subunit in all known glycoprotein hormones. Small amounts of Gal and Fuc residues were observed. In contrast, composition analysis of the recombinant insect cell hFSHβ subunit preparations revealed greater Gal than was detected in the FSHα hydrolysate. Insect cell-expressed FSHβ subunits possessed very high levels of Fuc in their hydrolysates (manuscript Table 3).

3.4 Peptide-N-glycanase sensitivity of hFSH subunit variants

PNGaseF digestions of several hFSH preparations were undertaken using Prozyme (Hayward, CA) Glyko PNGaseF kits because monoclonal antibody RFSH20 could not recognize reduced hFSHβ preparations after carboxymethylation. While alkylation with iodoacetamide permitted detection with RFSH20, recoveries of this derivative were lower, and reduced sensitivity in the Western blot combined to rule out its use in small-scale experiments. Denaturation of FSH or subunit samples in SDS and 2-mercaptoethanol followed by dilution with non-ionic detergent NP-40 should have permitted PNGaseF to remove glycans from all four potential N-glycosylation sites in FSH, however, some aggregation was noted, as immunoreactive material accumulated at the top of the gels (Figs. 7 and 8). Resistance to enzymatic deglycosylation appeared to be generally associated with the lower MW bands, such as hFSHβ^{21} and hFSHβ^{18}.

In pituitary hFSH$^{24/21}$, the hFSHβ^{24} band largely disappeared and a 15,000 M_r band appeared following PNGaseF digestion (Fig. 7A, lanes 1 and 2). While the hFSHβ^{21} band decreased in intensity, some remained. Because of aggregation in the PNGaseF-digested sample, it is difficult to determine if the reduced band density was due to aggregation rather than to loss of carbohydrate. The preparation of hypo-glycosylated hFSH$^{21/18}$ exhibited an unusual mobility such that it appeared to be composed largely of the hFSHβ^{18} band. After PNGaseF digestion,

some of this material continued to migrate at 18,000 M_r, while some appeared as the 15,000 M_r band, which appears to be fully deglycosylated hFSH (Fig. 7A, lane 4). Some hFSHβ^{24} and hFSHβ^{21} appeared in the PNGaseF-digested lane, but this could be carryover from lane 5. Urinary hFSH possessed slower migrating hFSHβ^{24} and hFSHβ^{21} bands, which have been reported previously (Bousfield et al., submitted). The hFSHβ^{24} band almost completely disappeared following PNGaseF digestion, as did most of the hFSHβ^{21} band. While three PNGaseF-resistant bands were observed, hFSHβ^{24}, hFSHβ^{21}, and hFSHβ^{18}, most of the immunoactivity appeared as the deglycosylated 15,000 M_r band. Recombinant GH_3-hFSH consisted of hFSHβ^{24} and hFSHβ^{21} bands before PNGaseF digestion and hFSHβ^{21} and hFSHβ^{15} bands after digestion. The α subunits in all hFSH preparations were completely PNGaseF-sensitive as all the immunoactive bands shifted from 20,000-23,000 M_r to 15,000 M_r. Despite the absence of significant aggregated immunoactivity at the top of the blot, the signal intensity of all PNGaseF-digested α subunit bands decreased, as if carbohydrate influenced HT13 antibody binding.

In a second experiment, PNGaseF digestion of recombinant GH_3-hFSH eliminated the hFSHβ^{24} band and partially eliminated the hFSHβ^{21} band (Fig. 8A). A pair of 15,000-16,000 M_r bands appeared, which were similar to those first observed for bacterially expressed hFSHβ (manuscript Fig. 6A). The GH_3-hFSHβ subunit fraction appeared to consist exclusively of the hFSHβ^{24} band, which completely disappeared after PNGaseF digestion, although proteolytic nicking produced a doublet near M_r 10,000. The fragment intensities and mobilities were unaffected by PNGaseF, consistent with monoclonal antibody RFSH20 recognizing an epitope in the non-glycosylated hFSHβ C-terminal fragment. The presence of hFSHβ subunit fragments has also been observed in pituitary hFSH subunit preparations as well (manuscript Fig. 2A). The completely deglycosylated GH_3-hFSHβ migrated as a 15,000 M_r band, with some 16,000 M_r band just visible. However, a hFSHβ^{21} band also appeared, suggesting some of the hFSHβ^{24} was partially resistant to PNGaseF digestion. This suggests an alternative interpretation of results seen in lanes 1 and 2. The hFSHβ^{21} band in lane 2 may have been derived from the hFSHβ^{24}

band, while the original hFSHβ^{21} band was converted into the 15,000 and 16,000 M_r bands. Gel filtration chromatography of recombinant mutant insect hFSH preparations identified heterodimer in only the βT26A preparation and we analyzed samples derived from both peaks. Both hFSHβ and hFSHα subunit bands were detected in the analysis of the βT26A dimeric peak sample, confirming the presence of FSH heterodimer. Only hFSHβ was observed in the subunit fraction. The absence of hFSHα indicated subunit dissociation took place prior to immunopurification with FSHβ-specific monoclonal antibody 46.3H6.B7, as dissociation during pH 2.7 elution would have produced a mixture of FSHβ and α subunits in the bound fraction. PNGaseF digestion resulted in only a small fraction of hFSHβ-T26A mutant migrating at 15,000 M_r. Both α mutant preparations, αT54A and αT80A, were found to consist of FSHβ subunit rather than FSH heterodimer by gel filtration (data not shown) and the absence of α subunit immunoactivity suggested FSH dissociated into subunits prior to elution from the antibody column. Both hFSHβ subunit bands exhibited reduced mobility, which increased to the same mobility as βT26A and αT54A bands by PNGaseF digestion. In addition, a distinct 15,000 M_r band was observed, although it represented a small portion of immunoactivity. The single glycosylation site mutant β-subunit insect hFSH preparation (βT26AhFSH) and its free FSHβT26A subunit were particularly resistant to enzymatic deglycosylation. As insect cell glycans often possess α1-3 linked fucose residues that inhibit PNGaseF, we performed carbohydrate analysis on several recombinant hFSH preparations including GH_3-hFSH, and all samples derived from the insect hFSH glycosylation mutants (manuscript Table 3). The results revealed 2.6 mol fucose per mol subunit in the most resistant insect hFSH mutant, βT26A. As this mutant possesses carbohydrate at a single glycosylation site, Asn^7, the average glycan possesses almost 3 fucose residues and PNGaseF resistance suggests two of these residues are core-linked. The α-subunit glycosylation site mutant-derived hFSHβ preparations possessed a somewhat lower fucose content than βT26A, but higher than GH_3-hFSH, consistent with their intermediate resistance to PNGaseF digestion. The disappearance of the hFSHβ^{21} band and appearance of the hFSHβ^{18} band was consistent with loss of a single glycan from most of the

preparation, while the hFSHβ^{15} band indicated complete deglycosylation of a fraction of the preparation (Fig. 7). The HT13 blot revealed total deglycosylation of hFSHα subunit, but the apparent affinity of the antibody for the subunit appeared to be reduced as indicated by densities only 11% those of the intact α subunit samples. Since the primary epitope for HT13 resides in αL3, near the Asn^{78} glycosylation site, the antibody may recognize carbohydrate as well as protein.

MALDI-MS of hFSH$^{21/18}$ subunit fractions indicated the presence of both non-glycosylated hFSHβ and a singly glycosylated hFSHβ. The signal for the former was not as strong as that reported several years ago for a hFSHβ^{21} preparation (Walton et al., 2001), while the latter resembled the signal for partially glycosylated eFSHβ (Bousfield et al., 1996). While hFSHβ synthesized in *Escherichia coli,* which lacked the N-glycosylation machinery, and PNGaseF digested hFSHβ produced the hFSHβ^{15} band, its absence in hFSH$^{21/18}$ Western blots was puzzling. It is possible that the weak signal in the MALDI-MS experiment resulted from low abundance, below the sensitivity of the Western blotting procedure. However, evidence for non-glycosylated hFSHβ in a hFSHβ^{21} preparation with no detectable hFSHβ^{15} included a very strong MALDI-MS signal for the non-glycosylated hFSHβ subunit (Walton et al., 2001).

4. References

Bousfield, G.R., Butnev, V.Y., Bidart, J.M., Dalpathado, D., Irungu, J. and Desaire, H., 2008. Chromatofocusing fails to separate hFSH isoforms on the basis of glycan structure, Biochemistry. 47, 1708-1720.

Bousfield, G.R., Butnev, V.Y., Gotschall, R.R., Baker, V.L. and Moore, W.T., 1996. Structural features of mammalian gonadotropins, Molec. Cell. Endocrinol. 125, 3-19.

Bousfield, G.R., Butnev, V.Y., Walton, W.J., Nguyen, V.T., Singh, V., Hueneidi, J., Kolli, K., Harvey, D.J. and Rance, N., 2007. All or none N-glycosylation in primate follicle-stimulating hormone β subunits, Molec. Cell. Endocrinol. 260-262, 40-48.

Bousfield, G.R. and Ward, D.N., 1984. Purification of lutropin and follitropin in high yield from horse pituitary glands, Journal of Biological Chemistry. 259, 1911-1921.

Dalpathado, D.S., Irungu, J.A., Go, E.P., Butnev, V.Y., Norton, K., Bousfield, G.R. and Desaire, H., 2006. Comparative glycomics of the glycoprotein hormone follicle-stimulating hormone (FSH): glycopeptide analysis of isolates from two mammalian species, Biochemistry. 45, 8665-8673.

Flack, M.R., Froehlich, J., Bennet, A.P., Anasti, J. and Nisula, B.C., 1994. Site-directed mutagenesis defines the individual roles of the glycosylation sites on follicle-stimulating hormone, J. Biol. Chem. 269, 14015-14020.

Fox, K.M., Dias, J.A. and Van Roey, P., 2001. Three-dimensional structure of human follicle-stimulating hormone, Molecular Endocrinology. 15, 378-389.

Green, E.D. and Baenziger, J.U., 1988. Asparagine-linked oligosaccharides on lutropin, follitropin, and thyrotropin II. distributions of sulfated and sialylated oligosaccharides on bovine, ovine, and human pituitary glycoprotein hormones, J. Biol. Chem. 263, 36-44.

Harvey, D.J., 2005. Fragmentation of negative ions from carbohydrates: part 3. Fragmentation of hybrid and complex N-linked glycans, J. Am. Soc. Mass Spectrom. 16, 647-659.

Harvey, D.J., Merry, A.H., Royle, L., Campbell, M.P., Dwek, R.A. and Rudd, P.M., 2009. Proposal for a standard system for drawing structural diagrams of N- and O-linked carbohydrates and related compounds, Proteomics. 9, 3796-3801.

Harvey, D.J., Royle, L., Radcliffe, C.M., Rudd, P.M. and Dwek, R.A., 2008. Structural and quantitative analysis of N-linked glycans by matrix-assisted laser desorption ionization and negative ion nanospray mass spectrometry, Anal. Biochem. 376, 44-60.

Louriero, R.F., de Oliveira, J.E., Torjesen, P.A., Bartolini, P. and Ribela, M.T.C.P., 2006. Analysis of intact human follicle-stimulating hormone preparations by reversed-phase high-performance liquid chromatography, J. Chromatogr. A. 1136, 10-18.

Renwick, A.G.C., Mizuochi, T., Kochibe, N. and Kobata, A., 1987. The asparagine-linked sugar chains of human follicle-stimulating hormone, J. Biochem. 101, 1209-1221.

Siegel, L.M. and Monty, K.J., 1966. Determination of molecular weights and frictional ratios of proteins in impure systems by use of gel filtration and density gradient centrifugation.

Application to crude preparations of sulfite and hydroxylamine reductase., Biochim. Biophys. Acta. 112, 346-362.

Stanton, P.G., Robertson, D.M., Burgon, P.G., Schmauk-White, B. and Hearn, M.T.W., 1992. Isolation and physicochemical characterization of human follicle-stimulating hormone isoforms, Endocrinology. 130, 2820-2832.

Walton, W.J., Nguyen, V.T., Butnev, V.Y., Singh, V., Moore, W.T. and Bousfield, G.R., 2001. Characterization of human follicle-stimulating hormone isoforms reveals a non-glycosylated β-subunit In addition to the conventional glycosylated β-subunit., J. Clin. Endocrinol. Metab. 86, 3675-3685.

5. Tables 1-6

Table 1. Amino acid sequence analysis of native hypo-glycosylated hFSH$^{21/18}$ by automated Edman degradation, showing results of the first 10 degradation cycles. The locations of the sequences are shown aligned to full-length α and β subunit sequences. The uppercase letters indicate PhNCS-amino acid derivatives detected by HPLC, while lower case letters show undetectable residues, in this case Cys residues, which are retained by disulfide bonds.

```
hFSHα
APDVQDCPECTLQENPLFSQPGAPILQCMGCCFSRAYPTPLRSKKTMLVQKNVTSESTCCVAKSYNRVTVMGGFKVENHTACHCSTCYYHKS
   VQDcPEcTLQEN
hFSHβ
NSCELTNITIAIEKEECRFCISINTTWCAGYCYTRDLVYKDPARPKIQKTCTFKELVYETVRVPGCAHHADSLYTYPVATQCHCGKCDSDSTDCTVRGLGPSYCSFGEMKE
  cELTNITIAIEK
NScELTNITIAI
```

Cycle	**1**	**2**	**3**	**4**	**5**	**6**	**7**	**8**	**9**	**10**
α seq	Val	Gln	Asp	(Cys)	Pro	Glu	(Cys)	Thr	Leu	Gln
Yield (pmol)	197.2	134.7	133.5	-	79.4	42.6	-	65.6	36.8	32.3
β seq	(Cys)	Glu	Leu	Thr	Asn	Ile	Thr	Ile	Ala	Ile
Yield (pmol)		79.0	69.0	53.1	7.8	51.1	65.6	70.7	40.0	70.7
β seq	Asn	Ser	(Cys)	Glu	Leu	Thr	Asn	Ile	Thr	Ile
Yield (pmol)	28.9	30.8	-	34.6	56.6	33.5	5.3	70.7	60.8	70.7

Table 2. Amino acid sequence analysis of hypo-glycosylated $hFSH^{21/18}$ subunit fraction by automated Edman degradation, showing results of the first 10 degradation cycles. The locations of the sequences are shown aligned to full-length α and β subunit sequences. The uppercase letters indicate PhNCS-amino acid derivatives detected by HPLC, while lower case letters show undetected residues, in this case Cys residues, which are retained by disulfide bonds.

```
hFSHα
APDVQDCPECTLQENPFFSQPGAPILQCMGCCFSRAYPTPLRSKKTMLVQKNVTSESTCCVAKSYNRVTVMGGFKVENHTACHCSTCYYHKS
   VQDcPEcTLQ

hFSHβ
NSCELTNITIAIEKEECRFCISINTTWCAGYCYTRDLVYKDPARPKIQKTCTFKELVYETVRVPGCAHHADSLYTYPVATQCHCGKCDSDSTDCTVRGLGPSYCSFGEMKE
  cELTNITIAI                                RPKIQKTcTf
NScELTNITI                                    QK
```

Cycle	**1**	**2**	**3**	**4**	**5**	**6**	**7**	**8**	**9**	**10**
αRes.	Val	Gln	Asp	(Cys)	Pro	Glu	(Cys)	Thr	Leu	Gln
Yield (pmol)	33.2	28.5	33.6	-	15.9	8.5	-	12.3	4.3	5.7
βRes.	Asn	Ser	(Cys)	Glu	Leu	Thr	Asn	Ile	Thr	Ile
Yield (pmol)	5.7	8.3	-	7.9	7.2	7.7	1.2	14.8	3.4	13.7
βRes.	(Cys)	Glu	Leu	Thr	Asn	Ile	Thr	Ile	Ala	Ile
Yield (pmol)	-	23.7	19.6	12.1	2.6	16.3	18.1	14.8	8.6	13.7
βRes.	Arg	Pro	Lys	Ile	Gln	Lys	Thr	(Cys)	Thr	Phe
Yield (pmol)	44.3	27.1	3.7	7.9	12.0	2.6	18.1	-	12.3	-
βRes	Gln	Lys								
Yield (pmol)	22.3	13.2								

Table 3, masses and compositions of the *N*-glycans found in hypo-glycosylated hFSH[21/18].

Neutral compounds							Structure[5]	Acidic compounds						
m/z ([M+H_2PO_4]$^-$ (Ion type a)[2]		Composition			Frag.[3]	%[4]		*m/z*		Acidic groups		Ion[2]	Frag.[3]	%[4]
Found	Calc.	Hex	HNAc	dHex				Found	Calc.	Neu5Ac	SO_3H			
1007.3	1007.3	3	2	0	+	5.10	1	-	-	-	-	-	-	-
1153.4	1153.4	3	2	1	+	4.82	2	-	-	-	-	-	-	-
1169.3	1169.3	4	2	0	-	0.74	3	-	-	-	-	-	-	-
1210.4	1210.4	3	3	0	+	1.95	4	-	-	-	-	-	-	-
1331.4	1331.4	5	2	0	+	11.67	5	-	-	-	-	-	-	-
1356.4	1356.5	3	3	1	+	2.41	6	-	-	-	-	-	-	-
1372.5	1372.5	4	3	0	+	0.96	7	1565.5	1565.5	1	0	b	+	1.74
1413.5	1413.5	3	4	0	+	1.69	8	1606.6	1606.6	1	0	b	-	0.77
1413.5	1413.5	3	4	0	+		8	1395.5	1395.4	0	1	b	+	1.13
1493.5	1493.5	6	2	0	+	11.20	9	-	-	-	-	-	-	-
1518.5	1518.5	4	3	1	+	0.95	10	1711.6	1711.6	1	0	b	+	0.97
1559.5	1559.5	3	4	1	+	2.84	11	-	-	-	-	-	-	-
1559.5	1559.5	3	4	1	+		12	1541.5	1541.5	0	1	b	-	0.37
1575.5	1575.5	4	4	0	+	0.64	13	1768.6	1768.6	1	0	b	-	0.54
1616.6	1616.6	3	5	0	+	0.85	14	1809.7	1809.7	1	0	b	-	0.32
1616.6	1616.6	3	5	0	+		15	1598.5	1598.5	0	1	b	-	0.41
1655.5	1655.5	7	2	0	+	7.31	16	-	-	-	-	-	-	-

1721.6	1721.6	4	4	1	+	0.78	17	1914.7	1914.7	1	0	b	+	0.47
1737.6	1737.6	5	4	0	+	0.30	18	1930.8	1930.7	1	0	b	-	0.32
								1110.4	1110.4	2	0	c	-	1.86
1762.6	1762.6	3	5	1	+	0.82	19	-	-	-	-	-	-	-
1762.6	1762.6	3	5	1	+		20	1744.6	1744.6	0	1	b	-	0.13
1778.7	1778.6	4	5	0	+	0.59	21	1971.8	1971.8	1	0	b	+	0.83
1778.7	1778.6	4	5	0	+		22	1760.6	1760.6	0	1	b	+	0.33
								1025.3	1025.3	1	1	c	-	2.34
								1130.9	1130.9	2	0	c	-	2.86
1817.6	1817.6	8	2	0	+	11.50	23	-	-	-	-	-	-	-
-	1819.6	3	6	0	-	-	24	2012.7	2012.7	1	-	b	-	0.08
-	1819.6	3	6	0	-	-	25	1045.8	1045.8	1	1	c	-	0.28
								940.3	940.3	0	2	c	-	1.14
1883.7	1883.6	5	4	1	+	0.38	26	2076.8	2076.8	1	-	b	+	0.24
								1183.4	1183.4	2	0	c	-	1.16
1924.7	1924.6	4	5	1	-	0.38	27	2117.8	2117.8	1	0	b	+	0.29
1924.7	1924.6	4	5	1	-		28	1906.7	1906.6	0	1	b	-	0.21
								1098.3	1098.3	1	1	c	-	1.59
1940.6	1940.7	5	5	0	+	0.26	29	2133.8	2133.8	1	0	b	+	0.25
								1211.9	1211.9	2	0	c	-	0.74
1965.7	1965.7	3	6	1	-	0.27	30	-	-	-	-	-	-	-
1965.7	1965.7	3	6	1	-		31	1947.7	1947.7	0	1	b	-	0.09
								1013.3	1013.3	0	2	c	-	1.14

1979.7	1979.6	9	2	0	+	4.85	32	-	-	-	-	-	-	-
-	1981.7	4	6	0	-	-	33	2174.8	2174.8	1	0	b	-	0.09
2029.6	2029.7	5	4	2	-	0.04	43-45	-	-	-	-	-	-	-
2070.7	2070.7	4	5	2	-	0.12	43-44[6]	2052.7	2052.7	0	1	a	-	0.18
2086.8	2086.7	5	5	1	+	0.22	34	2279.7	2279.8	1	0	b	+	0.13
								1285.0	1285.0	2	0	c	-	0.94
2102.7	2102.7	6	5	0	-	0.08	35	2295.8	2295.8	1	0	b	-	0.03
								1293.0	1293.0	2	0	c	-	0.29
2127.8	2127.7	4	6	1	-	0.09	36	2320.9	2320.8	1	0	b	-	0.02
2143.7	2143.7	5	6	0	+	0.12	37	2336.8	2336.8	1	0	b	-	0.03
								1313.4	1313.5	2	0	c	-	0.49
2232.8	2232.8	5	5	2	-	0.05	43-45[6]	-	-	-	-	-	-	-
2248.8	2248.8	6	5	1	-	0.07	38	2441.8	2441.9	1	0	b	-	0.03
								1366.0	1366.0	2	0	c	-	0.37
2289.8	2289.8	5	6	1	-	0.06	39	2482.9	2482.9	1	0	b	-	0.02
2305.8	2305.8	6	6	0	-	0.08	40	2498.9	2498.9	1	0	b	-	0.02
2451.8	2451.9	6	6	1	-	0.05	41	2644.7	2644.9	1	0	b	-	0.01
								1467.5	1467.5	2	0	c	-	0.27
2613.8	2613.9	7	6	1	-	0.02	42	-	-	-	-	-	-	-

(1) Compounds are listed in order of increasing mass of the neutral glycans. The masses for the acidic glycans that were found in the sample are listed after the neutral structures.
(2) Ions: a = $[M+H_2PO_4]^-$, b = $[M-H]^-$, c = $[M-2H]^{2-}$.
(3) + = confirmed by fragmentation.
(4) % of total identified glycans. T = trace.
(5) The numbers refer to the structure diagrams shown in Fig. 5.
(6) GalNAc means that a galactose residue has been replaced by GalNAc.

Table 4, *N*-Glycans found in hypo-glycosylated hFSH[21/18] after digestion with *Arthrobacter ureafaciens* sialidase.[1]

Neutral compounds						Structure[4]	Acidic compounds				
m/z ($[M+H_2PO_4]^-$ (Ion type a)[2]		Composition			Frag.[3]		*m/z*		SO_3H	Ion[2]	Frag.[3]
Found	Calc.	Hex	HexNAc	dHex			Found	Calc.			
1007.3	1007.3	3	2	0	+	1	-	-	-	-	-
1153.4	1153.4	3	2	1	+	2	-	-	-	-	-
1210.4	1210.4	3	3	0	+	4	-	-	-	-	-
1331.4	1331.4	5	2	0	+	5	-	-	-	-	-
1356.5	1356.5	3	3	1	+	6	-	-	-	-	-
1372.4	1372.5	4	3	0	+	7	-	-	-	-	-
1413.5	1413.5	3	4	0	+	8	-	-	-	-	-
1413.5	1413.5	3	4	0	+	8	1395.5	1395.5	1	b	+
1493.5	1493.5	6	2	0	+	9	-	-	-	-	-
1518.5	1518.5	4	3	1	+	10	-	-	-	-	-
1559.6	1559.5	3	4	1	+	11	-	-	-	-	-
1559.6	1559.5	3	4	1	+	12	1541.5	1541.6	1	b	-
1575.5	1575.5	4	4	0	+	13	-	-	-	-	-
1616.6	1616.6	3	5	0	+	14	-	-	-	-	-
1616.6	1616.6	3	5	0	+	15	1598.5	1598.6	1	b	-
1655.6	1655.6	7	2	0	+	16	-	-	-	-	-
1721.6	1721.6	4	4	1	+	17	-	-	-	-	-

1737.6	1737.6	5	4	0	+	18	-	-	-	-	-
1762.6	1762.6	3	5	1	+	19	-	-	-	-	-
1762.6	1762.6	3	5	1	+	20	1744.6	1744.6	1	b	-
1778.7	1778.6	4	5	0	+	21	-	-	-	-	-
1778.7	1778.6	4	5	0	+	22	1760.6	1760.6	1	b	+
1817.6	1817.6	8	2	0	+	23	-	-	-	-	-
-	1819.6	3	6	0	-	24	-	-	-	-	-
-	1819.6	3	6	0	-	25	940.2	940.3	2	c	-
1883.7	1883.6	5	4	1	+	26	-	-	-	-	-
1924.7	1924.6	4	5	1	-	27	-	-	-	-	-
1924.7	1924.6	4	5	1	-	28	1906.7	1906.6	1	b	-
19407	1940.7	5	5	0	+	29	-	-	-	-	-
1965.7	1965.7	3	6	1	-	30	-	-	-	-	-

1965.7	1965.7	3	6	1	-	31	1947.7	1947.7	1	b	-
							1013.3	1013.3	2	c	-
1979.7	1979.6	9	2	0	+	32	-	-	-	-	-
-	1981.7	4	6	0	-	33	-	-	-	-	-
2086.8	2086.7	5	5	1	+	34	-	-	-	-	-
2102.8	2102.7	6	5	0	-	35	-	-	-	-	-
2127.8	2127.7	4	6	1	-	36	-	-	-	-	-
2143.7	2143.7	5	6	0	+	37	-	-	-	-	-
2232.8	2232.8	5	5	2	-	43-45	-	-	-	-	-

2248.8	2248.8	6	5	1	-	38	-	-	-	-	-
2289.8	2289.8	5	6	1	-	39	-	-	-	-	-
2305.8	2305.8	6	6	0	-	40	-	-	-	-	-
2451.8	2451.9	6	6	1	-	41	-	-	-	-	-
2613.8	2613.9	7	6	1	-	42	-	-	-	-	-

(1) Compounds are listed in order of increasing mass of the neutral glycans. The masses for the acidic glycans that were found in the sample are listed after the neutral structures.

(2) Ions: a = $[M+H_2PO_4]^-$, b = $[M-H]^-$, c = $[M-2H]^{2-}$.

(3) + = confirmed by fragmentation.

(4) The numbers refer to the glycan structure diagrams in Fig. 5.

Table 5. Amino terminal amino acid sequence of hypo-glycosylated hFSHβ subunit.

```
hFSHβ
NSCELTNITIAIEKEECRFCISINTTWCAGYCYTRDLVYKDPARPKIQKTCTFKELVYETVRVPGCAHHADSLYTYPVATQCHCGKCDSDSTDCTVRGLGPSYCSFGEMKE
                                    YKDPARP_IQ
  cELTNITIAI
NScELTNITI
```

Cycle	**1**	**2**	**3**	**4**	**5**	**6**	**7**	**8**	**9**	**10**
Res.	Tyr	Lys	Asp	Pro	Ala	Arg	Pro	(Lys)	Ile	Gln
Yield (pmol)	41.4	11.8	32.9	33.0	18.7	27.0	16.1	-	18.8	10.6
Res.	(Cys)	Glu	Leu	Thr	Asn	Ile	Thr	Ile	Ala	Ile
Yield (pmol)	-	20.7	17.9	11.5	1.8	12.6	10.5	(13.6)	7.1	17.9
Res.	Asn	Ser	(Cys)	Glu	Leu	Thr	Asn	Ile	Thr	Ile
Yield (pmol)	5.7	4.4	-	4.9	5.0	4.1	0.6	(13.6)	4.9	(17.9)

Table 6. Amino terminal amino acid sequence of hypo-glycosylated hFSHα subunit.

hFSHα
APDVQDCPECTLQENPLFSQPGAPILQCMGCCFSRAYPTPLRSKKTMLVQKNVTSESTCCVAKSYNRVTVMGGFKVENHTACHCSTCYYHKS
VQDcP

Cycle	**1**	**2**	**3**	**4**	**5**	**6**	**7**	**8**	**9**	**10**
Res.	Val	Gln	Asp	(Cys)	Pro					
Yield (pmol)	12.0	10.3	10.2	-	2.4					

6. Figure Legends

Figure 1. Demonstration of a significant difference in size between fully- and hypo-glycosylated FSH glycoforms. A. Superdex 75 gel filtration of 1 μg fully-glycosylated hFSH. B. Superdex 75 gel filtration of 1 μg hypo-glycosylated hFSH. C. Superdex 75 gel filtration of 1 μg samples of each glycoform. Two 10 x 300 mm Superdex 75 columns were coupled in series. Each chromatogram was developed with 20% acetonitrile/0.2 M ammonium bicarbonate at a flow rate of 0.4 ml/min. UV absorbance was monitored at 210 nm. The retention times for molecular weight marker proteins are indicated with arrows and the molecular weight determined for each hFSH glycoform peak is indicated in each panel.

Figure 2. Nano-ESI mass spectrometry of hypo-glycosylated hFSH$^{21/18}$ glycans. A. Intact glycan negative ion nano-ESI spectrum. B. *Arthrobacter ureafaciens* sialidase-digested glycan negative ion nano-ESI spectrum. (Note 20 x magnification above *m/z* 2040). The results are further illustrated in Figs. 3 & 4 and tabulated in Tables 3 and 4.

Figure 3. Glycan structures derived from hypo-glycosylated hFSH. Only neutral core structures corresponding to 46 glycan ions in the desialylated glycan spectrum (Fig. 3B) are shown. In several cases two possible isobaric structures are illustrated. The diagrams follow the conventions of the Oxford Glycobiology Institute system (Harvey, Merry, Royle et al., 2009), except that hexose C6-linkages are shown as longer lines to emphasize the exocyclic position of the substituent (as well as providing space for bisecting GlcNAc residues in some diagrams). Three structures, 44-46, are not shown, but appear to be biantennary and to possess two fucose residues ± a single GalNAc residue.

Figure 4. Comparison of hypo-glycosylated hFSH glycans with pituitary hFSH glycans. Glycans removed from highly purified pituitary hFSH$^{24/21}$ obtained from the National Hormone and Pituitary Program were characterized by mass spectrometry, using the same methods

employed in this study and compared with those obtained from hypo-glycosylated $hFSH^{21/18}$ (Table 3). The relative abundances for oligosaccharide variants bearing the same neutral core glycan structure were combined for each bar. Structures of the more abundant cores are shown above.

Figure 5. Isolation of hypo-glycosylated hFSH subunits. The bound and unbound fractions of pooled subunit fractions were chromatographed over a 10 x 300 mm Superdex 75 column as described (manuscript Fig. 1). A. Unbound fraction possessing hypo-glycosylated $hFSH^{21/18}\alpha$. B. Bound fraction possessing hypo-glycosylated $hFSH^{21/18}\beta$.

Figure 6. MALDI-MS analysis of hypo-glycosylated hFSH subunits. A. $FSH^{21/18}\alpha$ subunit from Fig. 5A, above. Inset: SDS-PAGE of reduced samples of hypo-glycosylated $hFSH^{21/18}$ subunit preparations analyzed by MALDI-MS. Lane 1, MW markers, as indicated; lane 2, hFSHα; lane 3, hFSHβ. B. $FSH^{21/18}\beta$ subunit from Fig. 5B, above.

Figure 7. PNGaseF sensitivity in several pituitary hFSH preparations. A. FSHβ before and after PNGaseF digestion, as indicated, evaluated by Western blotting under denaturing conditions, probed with monoclonal antibody RFSH20. B. FSHα sensitivity to PNGaseF digestion under denaturing conditions probed with monoclonal antibody HT13. Lane 1, $hFSH^{24/21}$; lane 2, $hFSH^{24/21}$ + PNGaseF; lane 3, pituitary $hFSH^{21}$; lane 4, pituitary $hFSH^{21}$ +PNGaseF; lane 5, urinary $hFSH^{24/21}$; lane 6, urinary $hFSH^{24/21}$ +PNGaseF; lane 7, GH_3-$hFSH^{24/21}$; lane 8, GH_3-$hFSH^{24/21}$ +PNGaseF.

Fig. 8. PNGaseF sensitivity of several recombinant hFSH preparations. A. FSHβ sensitivity under denaturing conditions. B. FSHα sensitivity to PNGaseF digestion under denaturing conditions. One μg samples of each preparation were loaded in the same order in both blots. Lane 1, GH_3-hFSH; lane 2, GH_3-hFSH + PNGaseF; lane 3 GH_3-hFSHβ; lane 4, GH_3-hFSHβ + PNGaseF; lane 5, βT26A-hFSH; lane 6, βT26A-hFSH + PNGaseF; lane 7, βT26A-hFSHβ

subunit; lane 8, βT26A-hFSHβ subunit + PNGaseF; lane 9, αT54A-hFSHβ subunit; lane 10 αT54A-hFSHβ subunit + PNGaseF; lane 11, αT80A-hFSHβ subunit; lane 12 αT80A-hFSHβ subunit + PNGaseF.

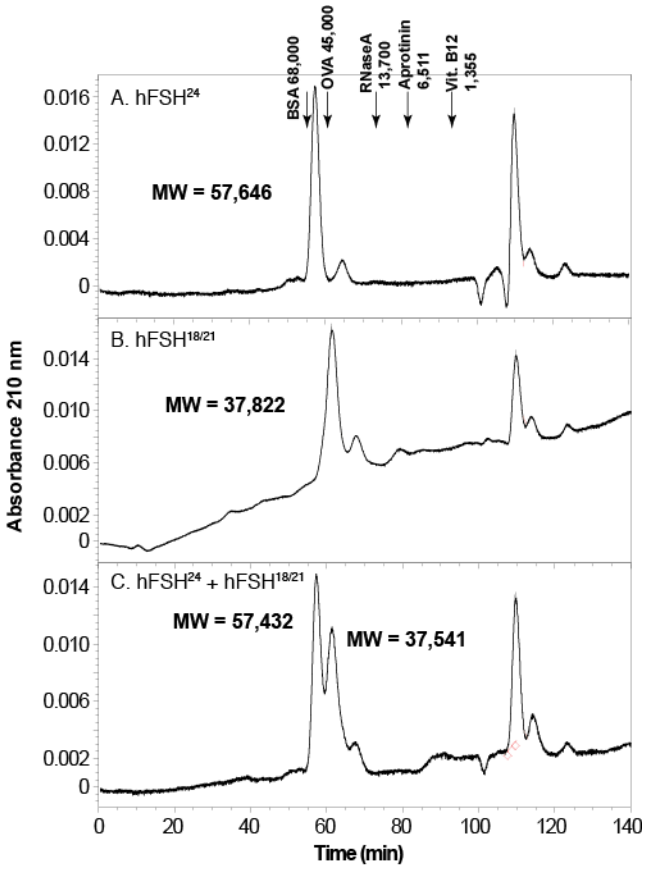
BSA 68,000
OVA 45,000
RNaseA 13,700
Aprotinin 6,511
Vit. B12 1,355
A. hFSH24
MW = 57,646
B. hFSH18/21
MW = 37,822
C. hFSH24 + hFSH18/21
MW = 57,432
MW = 37,541
Absorbance 210 nm
Time (min)

Figure 1.

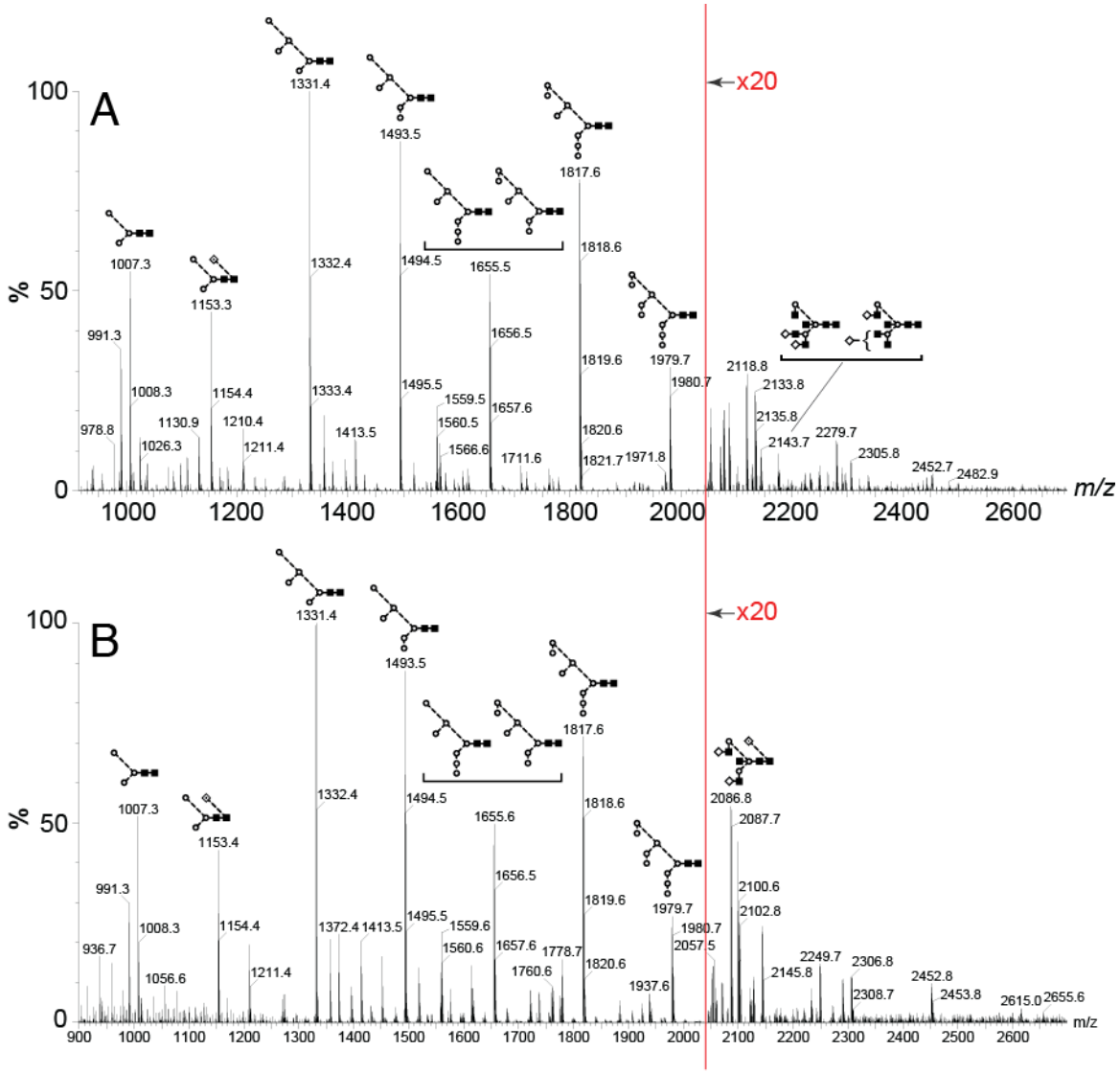
A
100
50
0
%
x20
1331.4
1493.5
1817.6
1007.3
1153.3
1332.4
1494.5
1655.5
1818.6
991.3
1656.5
1819.6
1979.7
1008.3
1154.4
1333.4
1495.5
1559.5
1980.7
2118.8
2133.8
978.8
1130.9
1210.4
1657.6
1560.5
2135.8
1026.3
1211.4
1413.5
1566.6
1820.6
2143.7
2279.7
1711.6
1821.7
1971.8
2305.8
2452.7
2482.9
1000
1200
1400
1600
1800
2000
2200
2400
2600
m/z
B
100
50
0
%
x20
1331.4
1493.5
1817.6
1007.3
1153.4
1332.4
1494.5
1655.6
1818.6
2086.8
2087.7
991.3
1656.5
1819.6
1979.7
2100.6
2102.8
1008.3
1154.4
1372.4
1413.5
1495.5
1559.6
1980.7
936.7
1560.6
1657.6
1778.7
1820.6
2057.5
1056.6
1211.4
1760.6
1937.6
2145.8
2249.7
2306.8
2308.7
2452.8
2453.8
2615.0
2655.6
900
1000
1100
1200
1300
1400
1500
1600
1700
1800
1900
2000
2100
2200
2300
2400
2500
2600
m/z

Figure 2.

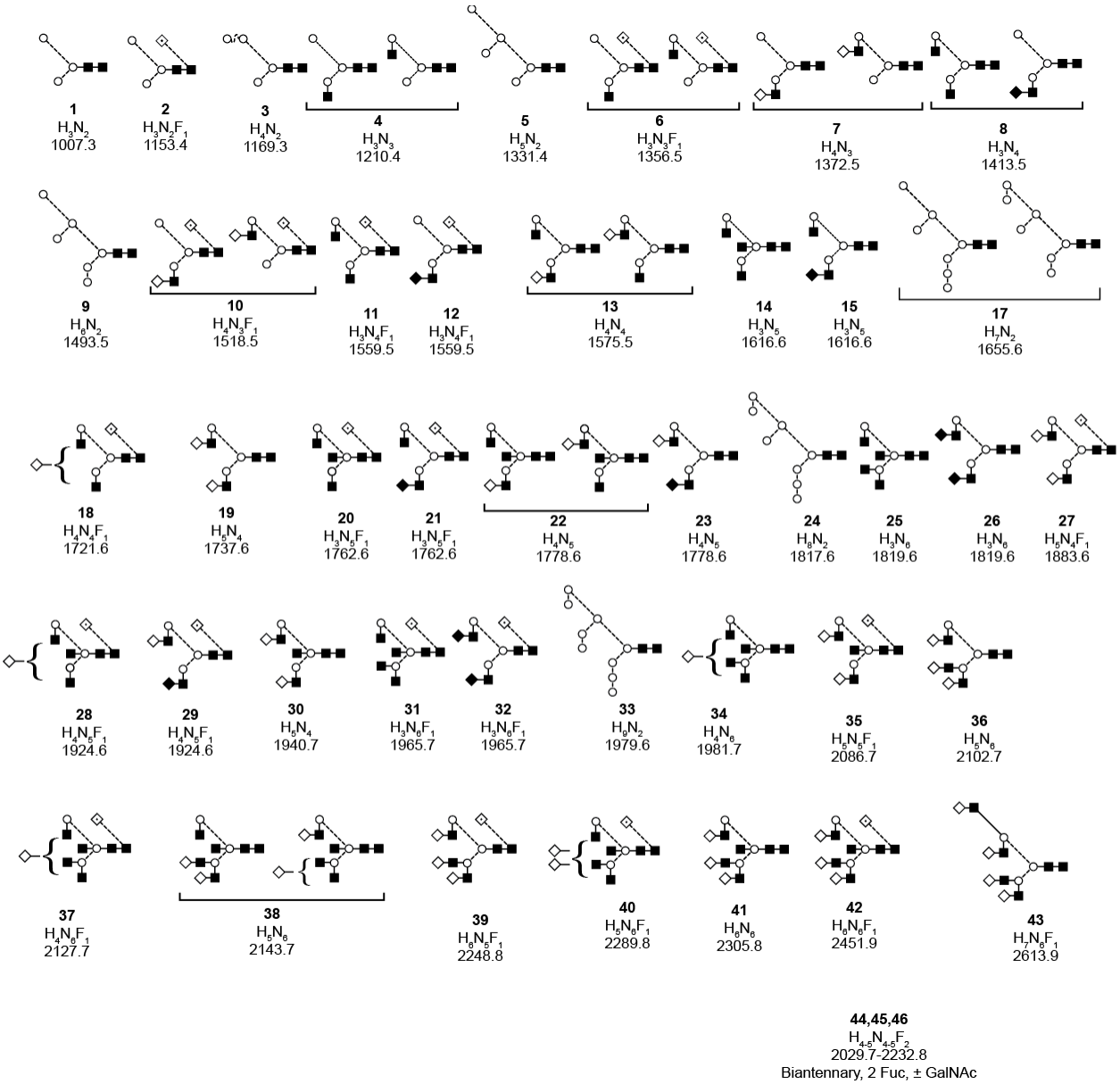
1
H3N2
1007.3
2
H3N2F1
1153.4
3
H4N2
1169.3
4
H3N3
1210.4
5
H5N2
1331.4
6
H3N3F1
1356.5
7
H4N3
1372.5
8
H3N4
1413.5
9
H6N2
1493.5
10
H4N3F1
1518.5
11
H3N4F1
1559.5
12
H3N4F1
1559.5
13
H4N4
1575.5
14
H3N5
1616.6
15
H3N5
1616.6
17
H7N2
1655.6
18
H4N4F1
1721.6
19
H5N4
1737.6
20
H3N5F1
1762.6
21
H3N5F1
1762.6
22
H4N5
1778.6
23
H4N5
1778.6
24
H8N2
1817.6
25
H3N6
1819.6
26
H3N6
1819.6
27
H5N4F1
1883.6
28
H4N5F1
1924.6
29
H4N5F1
1924.6
30
H5N4
1940.7
31
H3N6F1
1965.7
32
H3N6F1
1965.7
33
H8N2
1979.6
34
H4N6
1981.7
35
H5N5F1
2086.7
36
H5N6
2102.7
37
H4N6F1
2127.7
38
H5N6
2143.7
39
H6N5F1
2248.8
40
H5N6F1
2289.8
41
H6N6
2305.8
42
H6N6F1
2451.9
43
H7N6F1
2613.9
44,45,46
H4-5N4-5F2
2029.7-2232.8
Biantennary, 2 Fuc, ± GalNAc

Figure 3.

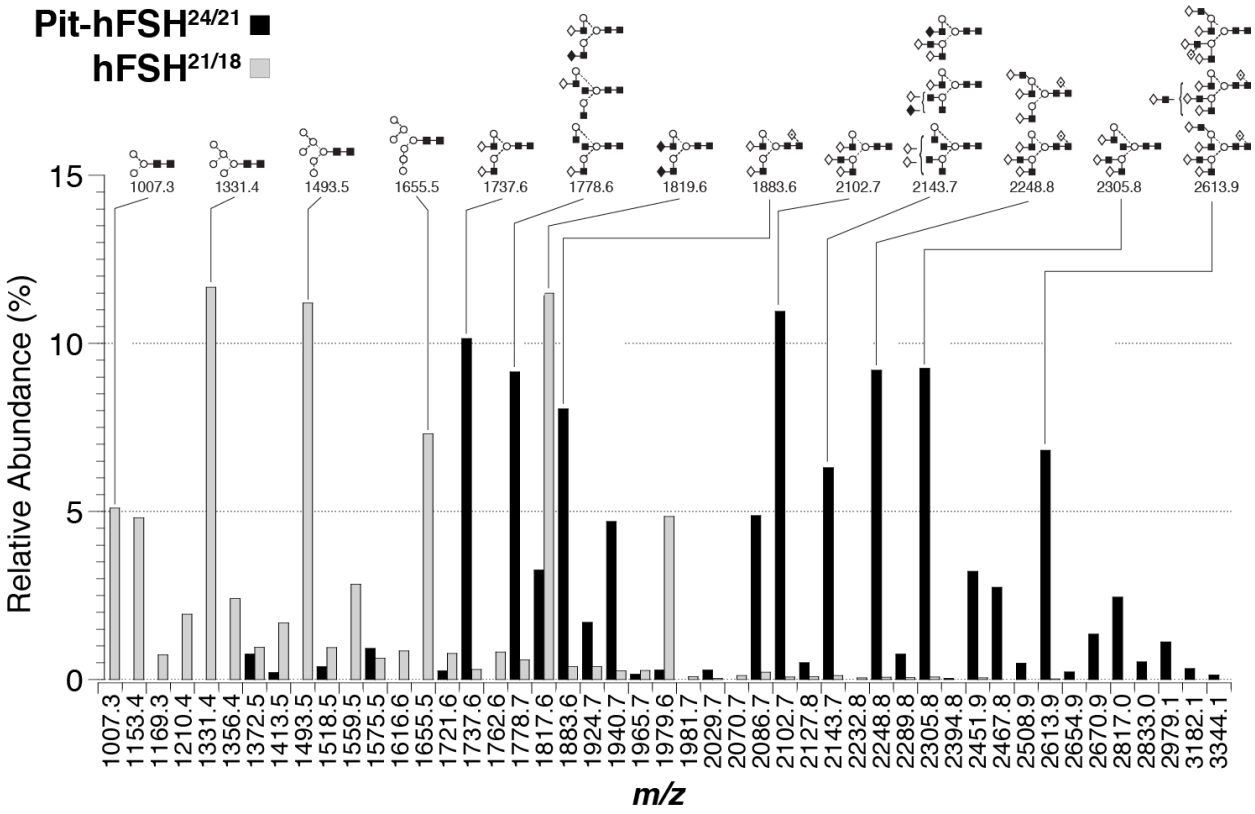
Pit-hFSH24/21
hFSH21/18
Relative Abundance (%)
m/z
1007.3
1331.4
1493.5
1655.5
1737.6
1778.6
1819.6
1883.6
2102.7
2143.7
2248.8
2305.8
2613.9

Figure 4.

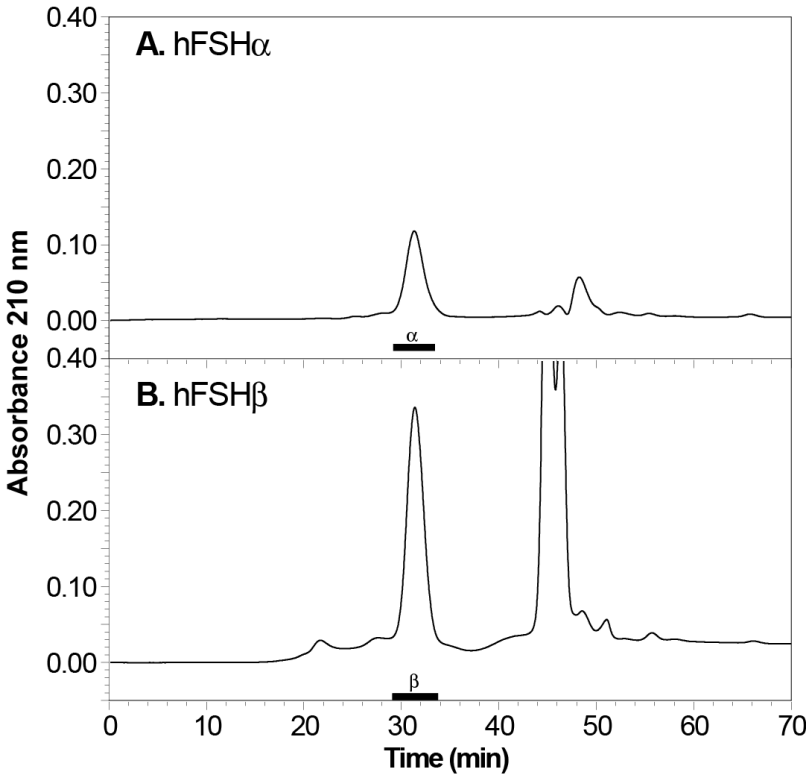
A. hFSHα
B. hFSHβ
α
β
Absorbance 210 nm
Time (min)
0.40
0.30
0.20
0.10
0.00
0
10
20
30
40
50
60
70

Figure 5.

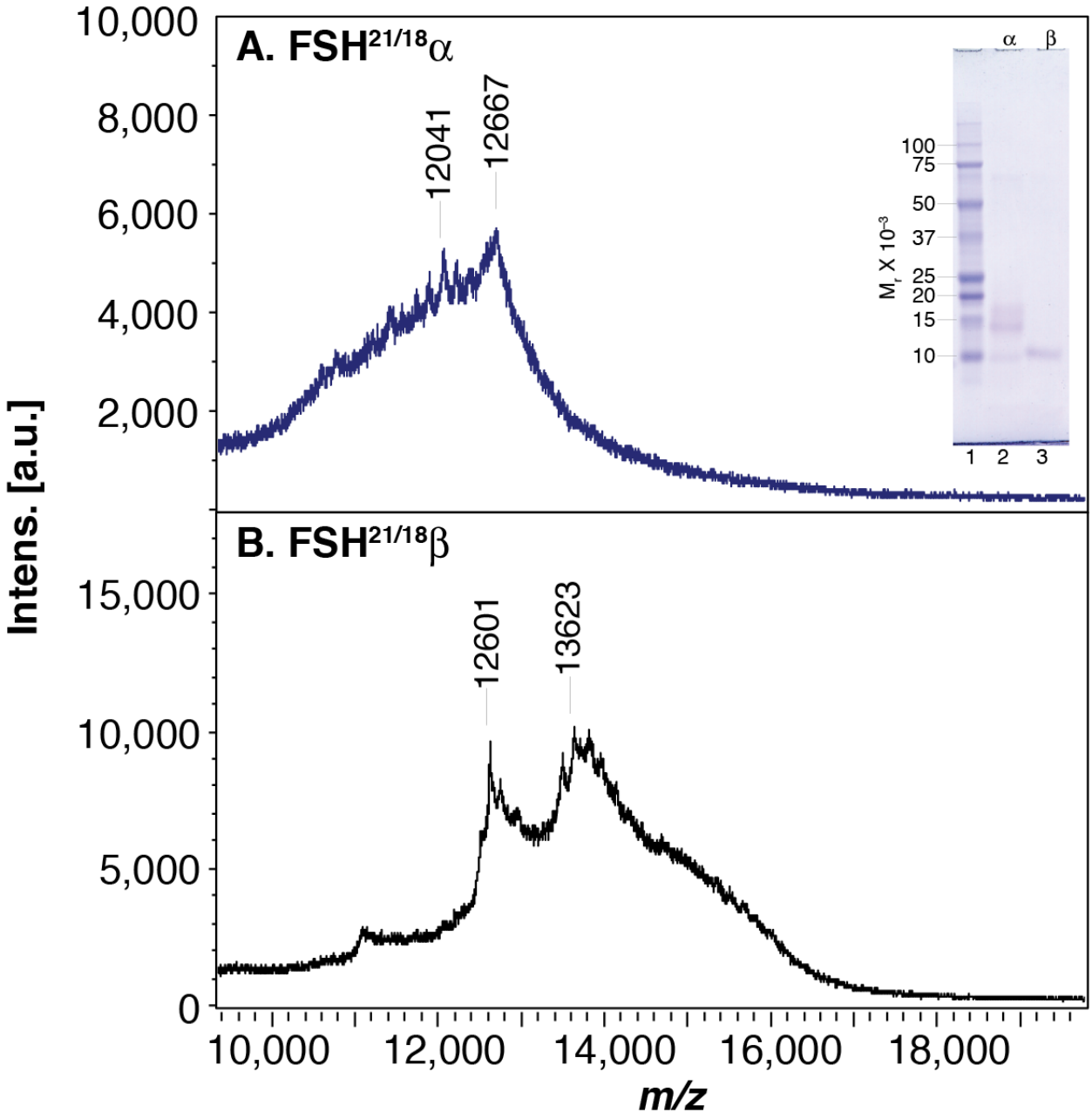
A. FSH21/18α
12041
12667
10,000
8,000
6,000
4,000
2,000
α
β
100
75
50
37
25
20
15
10
Mr X 10-3
1 2 3
B. FSH21/18β
12601
13623
15,000
10,000
5,000
0
Intens. [a.u.]
10,000
12,000
14,000
16,000
18,000
m/z

Figure 6.

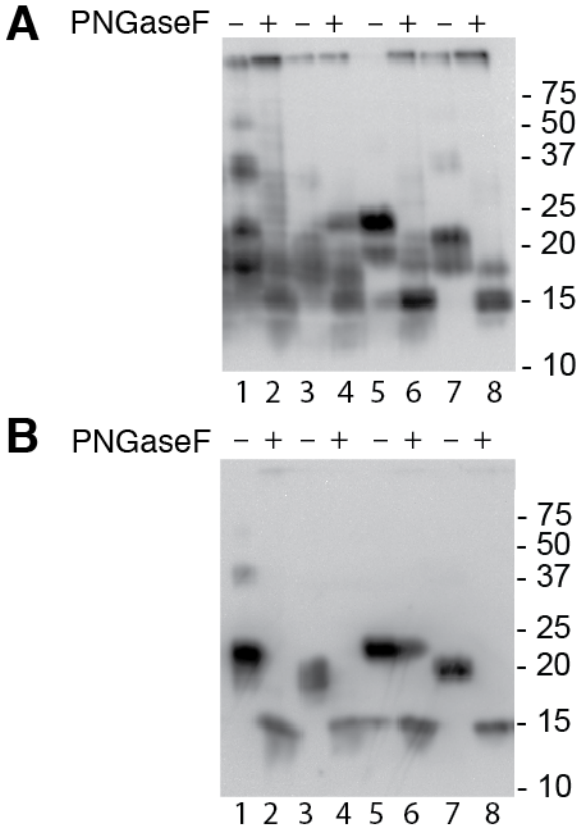
A
PNGaseF – + – + – + – +
- 75
- 50
- 37
- 25
- 20
- 15
- 10
1 2 3 4 5 6 7 8
B
PNGaseF – + – + – + – +
- 75
- 50
- 37
- 25
- 20
- 15
- 10
1 2 3 4 5 6 7 8

Figure 7.

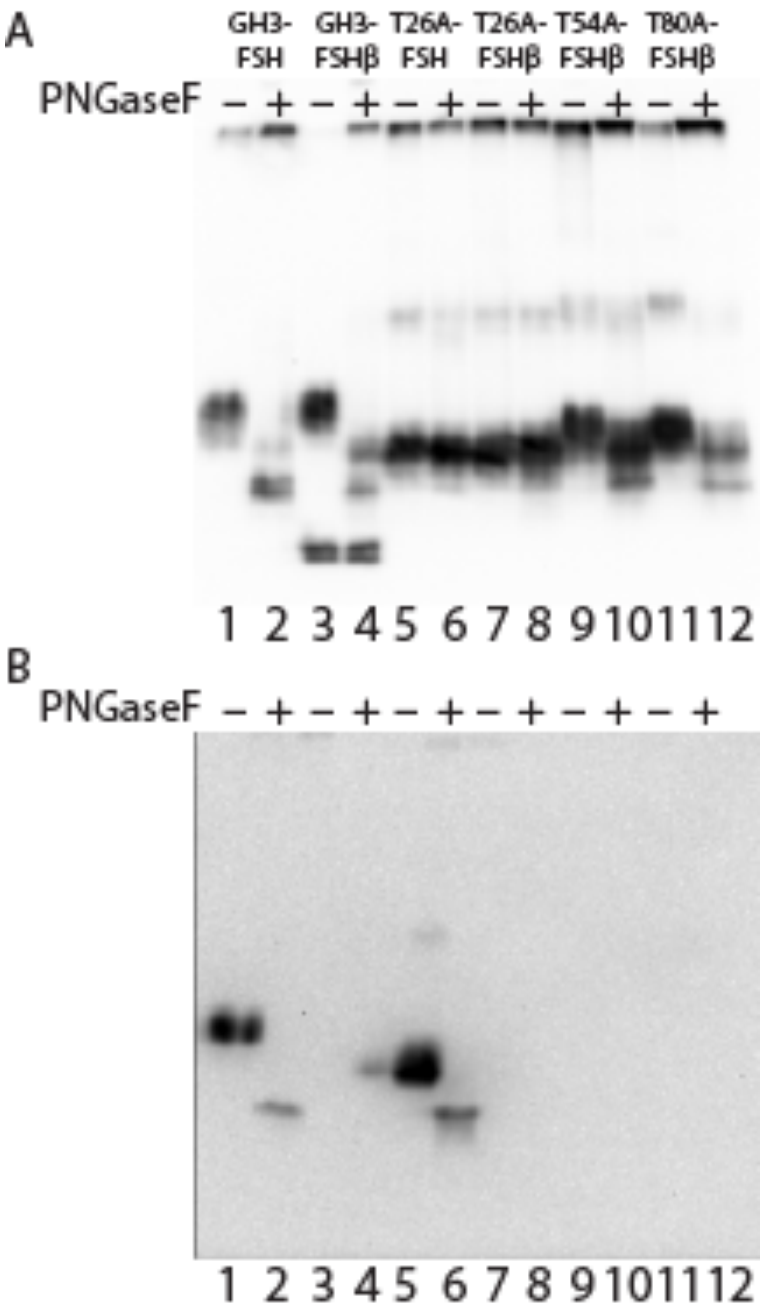
A
GH3-FSH
GH3-FSHβ
T26A-FSH
T26A-FSHβ
T54A-FSHβ
T80A-FSHβ
PNGaseF – + – + – + – + – + – +
1 2 3 4 5 6 7 8 9 10 11 12
B
PNGaseF – + – + – + – + – + – +
1 2 3 4 5 6 7 8 9 10 11 12

Figure 8.